Effect of a submerged or a surface piercing porous barrier on structure-coupled gravity waves

R. Ashok[a,*], M. Sivanesan[b], S.R. Manam[a]

[a] *Department of Mathematics, Indian Institute of Technology Madras, Chennai 600036*
[b] *Department of Mathematics, National Institute of Technology, Tiruchirappalli 620015*

Abstract

Flexural or membrane-coupled or capillary gravity wave scattering by a submerged or a piercing vertical porous barrier is analytically studied based on a connection that involves the solution potentials and few auxiliary potentials. The problems for the auxiliary potentials are relatively easy to handle for their solutions. The original problem is decomposed into two scattering or radiation problems of this type. The solution wave potential is determined in terms of those resolved wave potentials. Numerical results for the explicitly obtained scattering quantities are also presented.

2020 *Mathematics subject classification*: primary 76B15; secondary 35M12.
Keywords: potential, reflection coefficient, porous barrier, flexural gravity waves.

1. Introduction

The study of free surface gravity waves and their interaction with structures like ice-sheets, membranes and elastic plates plays a significant role in the design and the development of floating breakwaters and very large floating structures (VLFS) that are needed to protect offshore structures or to utilize the ocean space for humanitarian activities and military operations. It is known that membrane breakwaters have economic and environmental advantages over the elastic ones in coastal zones. On the other hand, VLFS have a major role in the offshore regions. One of the issues in the construction

*Corresponding author
Email address: ashokkumaraswin@gmail.com (R. Ashok)

of VLFS is curbing the undesirable plate deflections. By placing submerged structures at one end of or beneath the VLFS, these deflections are controlled [16-19]. In this context, it was also desirable to study the problem of flexural gravity wave interaction with a submerged ridge in polar oceans [12].

It is not uncommon to find many interesting studies on wave interactions with an ice-cover [4, 8]. Also, flexural gravity wave interactions with submerged bodies are semi-analytically studied by Das and Mandal [2, 3]. In particular, flexural wave interaction with an inclined submerged vertical solid barrier is studied by Maiti and Mandal [9] with the use of hyper singular integral equations. However, a very few analytical studies are available in the literature to deal with the boundary value problems associated with such problems. An explicit method of solution has been devised by Manam [10] and Manam and Kaligatla [12] to tackle the membrane-coupled or flexural gravity wave scattering by thin vertical solid barriers. Their solution method has special importance that is exhibited in capturing enhanced reflection at certain wave frequencies due to the presence of the floating structure and the partial vertical barrier. Using generalized expansion formula and associated orthogonal mode-coupling relation, Karmakar et al. [5] have analyzed the flexural gravity wave scattering problem involving multiple articulated floating elastic plates. Mondal and Sahoo [14, 15] have investigated flexural gravity wave interaction problem involving solid barriers in a two-layer or a three-layer fluid with finite and infinite water depths. Behera et al. [1] have studied oblique flexural gravity wave scattering by a finite submerged porous plate.

Free surface wave interactions with porous structures is an important study to understand the role of permeability in wave attenuation. Partial porous structures such as bottom-standing or surface piercing ones are usually considered in coastal applications for various reasons that pertain to navigation or the bottom condition. Not a single analytical solution procedure is available in the literature to tackle the scattering problem involving any partial porous structure until recently when Manam and Sivanesan [13] completely resolved the problem involving thin vertical porous barriers for normal wave incidence in deep water. The method of solution is based on the decomposition of the original problem into two explicitly solvable scattering or radiation problems involving a vertical solid barrier of same configuration.

In the present paper, the decomposition method of Manam and Sivanesan [13] is exploited to tackle the structure-coupled gravity wave scattering by a submerged or a surface piercing vertical porous barrier. The decomposed problems in the present paper are solved explicitly by the aid of a weakly singular integral equation. It is useful to study the present class of problems in the development of VLFS or floating breakwaters with an aim to control undesirable plate deflections and in coastal engineering applications. The floating elastic structure is considered with or without compression. Also, this study can be a model for the scattering of flexural gravity waves by a thin submarine porous ridge in polar oceans. In Sections 2 and 3, the mathematical problem and its decomposition with the help of integral relations between the wave potentials associated with the original and the decomposed problems involving either the submerged or the surface piercing barrier. Moreover, explicit solutions of the decomposed problems are obtained in Sections 2 and 3 for flexural or ice-coupled as well as capillary or membrane-coupled gravity wave problems involving the barriers. Numerical results that describe the effect of the porous barrier on these structure-coupled gravity waves are presented along with conclusions in Sections 4 and 5.

2. Mathematical problem and its solution approach for submerged porous barrier case

A two-dimensional irrotational wave motion is considered in an inviscid incompressible fluid of infinite depth. Cartesian coordinates (x, y) are chosen with $y = 0$ being mean free surface and y pointing vertically downwards. A uniformly extended submerged thin vertical porous barrier is positioned at $x = 0, y \in B = (a, \infty)$, where B denotes the barrier position. The linearized wave motion can be represented by a time-harmonic velocity potential $\Phi_j(x, y, t) = \mathrm{Re}\left\{\hat{\phi}_j(x, y)\mathrm{e}^{(-1)^j \mathrm{i}\omega t}\right\}$, $j = 1, 2$, where $\Phi_j(x, y, t)$ with $j = 1$ and $j = 2$ represent the velocity potential associated with the incoming wave traveling from $x = +\infty$ and $x = -\infty$ respectively and ω is the incident wave frequency. Then, the velocity potential $\hat{\phi}_j(x, y)$, $j = 1, 2$ satisfies

$$\frac{\partial^2 \hat{\phi}_j}{\partial x^2} + \frac{\partial^2 \hat{\phi}_j}{\partial y^2} = 0, \quad -\infty < x < \infty, y > 0. \tag{1}$$

The boundary condition at undisturbed plate or ice-covered surface is given by

$$D\frac{\partial^5 \hat{\phi}_j}{\partial y^5} + M\frac{\partial^3 \hat{\phi}_j}{\partial y^3} + \frac{\partial \hat{\phi}_j}{\partial y} + K\hat{\phi}_j = 0, \quad \text{on} \quad y = 0 \; j = 1, 2, \tag{2}$$

where $D = EI/(\rho g - \rho_i d\omega^2)$, $M = \tau/(\rho g - \rho_i d\omega^2)$ and $K = \rho\omega^2/(\rho g - \rho_i d\omega^2)$. $EI = Ed^3/12(1-\nu^2)$-denotes flexural rigidity of the plate/ice-sheet, E-Young modulus, ν-Poisson ratio, $\rho-$density of water, ρ_i-mass density of the ice-sheet, d-thickness of the plate/ice-sheet, the flexible plate is under compression if $\tau < 0$ and tension if $\tau > 0$ (see Manam and Kaligatla [12]).
When the surface is covered with a membrane of thickness m, the boundary condition (2) becomes third order condition with $D = 0$, $M = \tau/(\rho g - m\omega^2)$ and $K = \rho\omega^2/(\rho g - m\omega^2)$, where τ is the membrane tension. When the free surface is considered with surface tension τ, the boundary condition (2) becomes with $D = 0, M = \tau/\rho g$ and $K = \omega^2/g$ (see Manam [10]).
The condition on the submerged vertical porous barrier is obtained as

$$\frac{\partial\hat{\phi}_j}{\partial x}(0^{\pm}, y) = (-1)^j \mathrm{i}\lambda\Gamma[\hat{\phi}_j(0^+, y) - \hat{\phi}_j(0^-, y)], \quad y \in (a, \infty),\ j = 1, 2, \tag{3}$$

where Γ is the non-dimensional complex porous effect parameter such that $\Gamma = \gamma(s_1 + \mathrm{i}s_2)/[\lambda d(s_1^2 + s_2^2)]$ in which γ is porosity constant, d is plate thickness, s_1 is resistance force coefficient, s_2 is inertial force coefficient,and λ is incident wave number (see Yu and Chwang [20]).
Since the fluid flow is continuous across the gap $x = 0, y \in G = (0, a)$, where G denotes gap position, the potential $\hat{\phi}_j,\ j = 1, 2$ must satisfy

$$\hat{\phi}_j(0^-, y) = \hat{\phi}_j(0^+, y), \quad y \in (0, a). \tag{4}$$

Absence of the fluid motion at large depth suggest that

$$|\nabla\hat{\phi}_j| \to 0, \quad \text{as} \quad y \to \infty,\ j = 1, 2. \tag{5}$$

The radiating conditions are specified as

$$\hat{\phi}_j(x, y) \sim \begin{cases} \phi^0(-x, y) + R_p\ \phi^0(x, y), & (-1)^{j+1}x \to \infty, \\ T_p\ \phi^0(-x, y), & (-1)^{j+1}x \to -\infty, \end{cases} \tag{6}$$

where $\phi^0(x, y) = \mathrm{e}^{\mathrm{i}\lambda x - \lambda y}$ represents an incident wave with λ being the positive real root of the dispersion equation $Dx^5 + Mx^3 + x - K = 0$ and R_p, T_p are reflection, transmission amplitudes of an incident wave respectively.
The potential function $\hat{\phi}_j$ $j = 1, 2$ has the edge behavior

$$|\nabla\hat{\phi}_j| \sim r^{-1/2}, \quad \text{as} \quad r \to 0. \tag{7}$$

where r is the local radius from the edge point $x = 0,\ y = a$ (see Karp and Karal [6]).
Since the horizontal velocity of the fluid is continuous across $x = 0$, one could reduce the upper-half plane problem for the potentials $\hat{\phi}_j(x, y), j = 1, 2$ into a quarter-plane problem. This is done by writing

$$\hat{\phi}_j(x,y) = \begin{cases} \phi^0(-x,y) + \phi^0(x,y) + \phi_j^p(x,y), & (-1)^j x < 0, \\ -\phi_j^p(-x,y), & (-1)^j x > 0, \ \text{for } j = 1, 2. \end{cases}$$

The new functions $\phi_1^p(x, y)$ and $\phi_2^p(x, y)$ are defined in the domain $x > 0$ and $x < 0$ respectively.
Therefore, if the functions $\phi_j^p(x, y), j = 1, 2$ is found then by using the above relation, it can be obtained the potential functions of original problem $\hat{\phi}_j(x, y), j = 1, 2$. Now, the new potential functions $\phi_j^p(x, y), j = 1, 2$ satisfy (1), (2), (5) and the boundary conditions

$$\frac{\partial \phi_j^p}{\partial x}(0,y) + 2\mathrm{i}\Gamma\lambda\Big(\phi_j^p(0,y) + \phi^0(0,y)\Big) = 0, \text{for } y \in (a,\infty), j = 1, 2,$$

$$\phi_j^p(0,y) + \phi^0(0,y) = 0, \quad y \in (0,a), j = 1, 2 \tag{8}$$

and

$$\phi_j^p(x,y) \to (R_p - 1)\phi^0(x,y) \ \text{ as } \ (-1)^j x \to -\infty, \quad j = 1, 2$$

with $T_p = 1 - R_p$.
The porous barrier edge condition (7) satisfied by $\hat{\phi}_j(x, y), j = 1, 2$ suggests that

$$|\nabla \phi_j^p| \sim r^{-1/2}, \quad \text{as} \ \ r \to 0, j = 1, 2. \tag{9}$$

When the porous barrier becomes a solid barrier, that is $\Gamma = 0$, the quarter-plane porous wave potentials $\phi_j^p(x, y), j = 1, 2$ reduce to solution potentials for wave scattering by the submerged solid barrier. These potentials are solid wave potentials and are denoted by $\phi_j(x, y), j = 1, 2$. They satisfy (1)-(2), (8)-(9) and the Neumann boundary condition

$$\frac{\partial \phi_j}{\partial x}(0,y) = 0, \text{for } y \in (a,\infty), j = 1, 2.$$

Also, radiation conditions are modified in this case as

$$\phi_j(x,y) \to (R - 1)\phi^0(x,y) \ \text{ as } \ (-1)^j x \to -\infty, \quad j = 1, 2,$$

where R is the reflection amplitude of an incident wave due to the solid barrier.

2.1. connection between the porous and the solid wave potentials

The connection takes the same form as the one in Manam and Sivanesan [13] that has been established for free surface gravity waves. It is an integral relation among the functions $\phi_j^p, \phi_j, j = 1, 2$ and the auxiliary wave potential functions $\psi_j, j = 1, 2$ as given by

$$\phi_j^p(x, y) + \mathrm{i}\lambda\Gamma \int_0^x \Big[\{\phi^0(t, y) + \phi^0(-t, y)\} + \sum_{m=1}^{2} \phi_m^p((-1)^{j+m}t, y)\Big] dt$$
$$= \phi_j(x, y) + \psi_j(x, y), (-1)^{j+1}x > 0, j = 1, 2. \quad (10)$$

Each term in the above connection is shown to satisfy Laplace equation. Also, it helps to decompose the original problem for $\phi_j^p(x, y)$ into two problems for the functions ϕ_j and ψ_j. The reader is referred to Manam and Sivanesan [13] for more details. Then, the problem for $\phi_j, j = 1, 2$ is merely scattering of structure-coupled waves by the submerged vertical solid barrier while the problem for the auxiliary potentials $\psi_j, j = 1, 2$ satisfy (1)-(2), (5) along with the conditions

$$\psi_j(0, y) = 0, \quad y \in (0, a), \quad (11)$$
$$\psi_{j_x}(0, y) = 0, \quad y \in (a, \infty) \quad (12)$$

and

$$\psi_j(x, y) \sim R_1^j\ \phi^0(x, y) + R_2^j\ \phi^0(-x, y), \ \ (-1)^{j+1}x \to \infty,$$

where $R_k^j, k = 1, 2$ are unknown constants.
Adding the relations in (10) after rewriting them in the same domain $x > 0$ and then make use of the addition in (10) produce the porous wave potentials $\phi_j(x, y), j = 1, 2$ in an explicit form as given by

$$\phi_j^p(x, y) = [\phi_j(x, y) + \psi_j(x, y)] - \Gamma[\phi^0(x, y) - \phi^0(-x, y)] -$$
$$\mathrm{i}K\Gamma \sum_{l=1}^{2} \int_0^x \Big[\phi_l((-1)^{j+l}t, y) + \psi_l((-1)^{j+l}t, y)\Big] dt, (-1)^{j+1}x > 0, j = 1, 2. \quad (13)$$

Now, it is only remained to explicitly solve the decomposed boundary value problems for ϕ_j and $\psi_j, j = 1, 2$. Their details are given in the next section.

2.2. Determination of the decomposed wave potentials

2.2.1. flexural or ice-coupled gravity wave scattering

We consider a problem for the function $\chi(x,y), x>0, y>0$ that satisfies (1)-(2), (5), (11), (12) and the radiating condition

$$\chi(x,y) \sim \eta_1\ \phi^0(x,y) + \eta_2\ \phi^0(-x,y), \text{ as } x \to \infty. \tag{14}$$

The general solution $\chi(x,y)$ that satisfies (1)-(2), (5) and (14) can be written as (see Manam and Kaligatla [12])

$$\chi(x,y) = \eta_1 e^{i\lambda x - \lambda y} + \eta_2 e^{-i\lambda x - \lambda y} + A_1 e^{i\lambda_1 x - \lambda_1 y} + A_2 e^{-i\bar{\lambda}_1 x - \bar{\lambda}_1 y} + \int_0^\infty A(\xi)\ L(\xi,y)\ e^{-\xi x}\, d\xi, \quad x>0, y>0,$$

where η_1, η_2, A_1, A_2, $A(\xi)$ are unknowns, $L(\xi,y) = \xi(1-M\xi^2+D\xi^4)\cos\xi y - K\sin\xi y$ and the roots of the polynomial equation $Dx^5+Qx^3+x-K=0$ are $\lambda, \lambda_j, \bar{\lambda}_j, j=1,2$. It is not difficult to see that $\lambda>0, \mathrm{Re}(\lambda_1)>0$ and $\mathrm{Re}(\lambda_2)<0$.

Application of the boundary conditions (11) and (12) produces a pair of integral equations

$$\mathscr{L}\int_0^\infty A(\xi)\ \sin\xi y\, d\xi = -(\eta_1+\eta_2)\, e^{-\lambda y} - A_1 e^{-\lambda_1 y} - A_2 e^{-\bar{\lambda}_1 y},\ y\in(0,a)$$

and

$$\mathscr{L}\int_0^\infty \xi A(\xi)\ \sin\xi y\, d\xi = (\eta_1-\eta_2) i\lambda e^{-\lambda y} + i\lambda_1 A_1 e^{-\lambda_1 y} - i\bar{\lambda}_1 A_2 e^{-\bar{\lambda}_1 y},\ y\in(a,\infty),$$

where $\mathscr{L} = (D\frac{\partial^5}{\partial y^5} + M\frac{\partial^3}{\partial y^3} + \frac{\partial}{\partial y} - K)$.

These are integrated to find that

$$\int_0^\infty A(\xi)\ \sin\xi y\, d\xi = C_1\, e^{\lambda y} + C_2\, e^{\lambda_1 y} + C_3\, e^{\bar{\lambda}_1 y} + C_4\, e^{\lambda_2 y} + C_5\, e^{\bar{\lambda}_2 y} + \frac{(\eta_1+\eta_2)}{S(\lambda)} e^{-\lambda y} + \frac{A_1}{S(\lambda_1)} e^{-\lambda_1 y} + \frac{A_2}{S(\bar{\lambda}_1)} e^{-\bar{\lambda}_1 y} \equiv f(y),\ y\in(0,a) \tag{15}$$

and

$$\int_0^\infty \xi A(\xi)\ \sin\xi y\, d\xi = D_1\, e^{\lambda_2 y} + D_2\, e^{\bar{\lambda}_2 y} + D_3\, e^{\lambda_1 y} + D_4\, e^{\bar{\lambda}_1 y} + D_5\, e^{\lambda y} - \frac{i\lambda}{S(\lambda)}(\eta_1-\eta_2) e^{-\lambda y} - \frac{i\lambda_1}{S(\lambda_1)} A_1 e^{-\lambda_1 y} + \frac{i\bar{\lambda}_1}{S(\bar{\lambda}_1)} A_2 e^{-\bar{\lambda}_1 y} \equiv h(y),\ y\in(a,\infty), \tag{16}$$

where $C_j, D_j, j = 1, 2, 3, 4, 5$ are arbitrary constants and $S(X) = X(1 + MX^2 + DX^4) + K$.
Since the Fourier integral (15) tends to 0 as $y \to 0$ and it is differentiable at least four more times, it may be obtained from (15) that

$$C_1 + C_2 + C_3 + C_4 + C_5 + \frac{1}{S(\lambda)}\eta_1 + \frac{1}{S(\lambda)}\eta_2 + \frac{1}{S(\lambda_1)}A_1 + \frac{1}{S(\bar{\lambda}_1)}A_2 = 0, \quad (17)$$

$$\lambda^2 C_1 + \lambda_1^2 C_2 + \bar{\lambda}_1^2 C_3 + \lambda_2^2 C_4 + \bar{\lambda}_2^2 C_5 + \frac{\lambda^2}{S(\lambda)}\eta_1 + \frac{\lambda^2}{S(\lambda)}\eta_2 + \frac{\lambda_1^2}{S(\lambda_1)}A_1 + \frac{\bar{\lambda}_1^2}{S(\bar{\lambda}_1)}A_2 = 0, \quad (18)$$

$$\lambda^4 C_1 + \lambda_1^4 C_2 + \bar{\lambda}_1^4 C_3 + \lambda_2^4 C_4 + \bar{\lambda}_2^4 C_5 + \frac{\lambda^4}{S(\lambda)}\eta_1 + \frac{\lambda^4}{S(\lambda)}\eta_2 + \frac{\lambda_1^4}{S(\lambda_1)}A_1 + \frac{\bar{\lambda}_1^4}{S(\bar{\lambda}_1)}A_2 = 0. \quad (19)$$

Also, since $h(y) \to 0$ as $y \to \infty$, the constants $D_3 = D_4 = 0$.
By the inversion of the Fourier sine transform (16), it may be obtained that

$$A(\xi) = \frac{2}{\pi\xi}\int_0^\infty P(y)\ \sin\xi y\, dy, \quad (20)$$

where

$$P(y) = \begin{cases} g_1(y), & \text{for } y \in (0, a) \\ h(y), & \text{for } y \in (a, \infty) \end{cases}$$

with

$$g_1(y) = \int_0^\infty \xi A(\xi)\ \sin\xi y\, d\xi,\ \ y \in (0, a).$$

Now, substituting $A(\xi)$ in the integral relation (15), one may obtain the weakly singular integral equation

$$\frac{1}{\pi}\int_a^\infty g_1(u)\log\left|\frac{u+x}{u-x}\right| du = f_1(x), \quad x \in (a, \infty), \quad (21)$$

where

$$f_1(x) = f(x) - \frac{1}{\pi}\int_a^\infty h(t)\log\left|\frac{x+t}{x-t}\right| dt.$$

Due to the fact that the pair of integral relations (15) and (16) are differentiable at least for four times, one can obtain a pair of weakly singular integral equations by applying the above procedure again and it may be obtained as

$$\frac{1}{\pi}\int_a^\infty g_j(u)\log\left|\frac{u+x}{u-x}\right|du = f_j(x), \quad x\in(a,\infty), \tag{22}$$

where

$$g_j(y) = \frac{d^{2(j-1)}g_1}{dy^{2(j-1)}}, \quad f_j(x) = \frac{d^{2(j-1)}f}{dx^{2(j-1)}} - \frac{1}{\pi}\int_a^\infty \frac{d^{2(j-1)}h}{dt^{2(j-1)}}\log\left|\frac{x+t}{x-t}\right|dt, j=2,3.$$

By applying the above process, $A(\xi)$ in (20) can be written as two more different integral forms. Then equate these $A(\xi)$ recursively, one may obtain the following conditions

$$h(a)=0,\ h''(a)=0,\ g_1'(a)=h'(a)\ \text{ and }\ g_1'''(a)=h'''(a).$$

The first two of the above conditions become

$$e^{\lambda_2 a}D_1 + e^{\bar{\lambda}_2 a}D_2 - \frac{i\lambda}{S(\lambda)}e^{-\lambda a}\eta_1 + \frac{i\lambda}{S(\lambda)}e^{-\lambda a}\eta_2 - \frac{i\lambda_1}{S(\lambda_1)}e^{-\lambda_1 a}A_1 + \frac{i\bar{\lambda}_1}{S(\bar{\lambda}_1)}e^{-\bar{\lambda}_1 a}A_2 = 0 \tag{23}$$

and

$$\lambda_2^2 e^{\lambda_2 a}D_1 + \bar{\lambda}_2^2 e^{\bar{\lambda}_2 a}D_2 - \frac{i\lambda^3}{S(\lambda)}e^{-\lambda a}\eta_1 + \frac{i\lambda^3}{S(\lambda)}e^{-\lambda a}\eta_2 - \frac{i\lambda_1^3}{S(\lambda_1)}e^{-\lambda_1 a}A_1 + \frac{i\bar{\lambda}_1^3}{S(\bar{\lambda}_1)}e^{-\bar{\lambda}_1 a}A_2 = 0. \tag{24}$$

The solution to the integral equations (21) and (22) subject to the bounded behavior of the functions $g_j(u), j=1,2,3$ at $u=a$ is obtained as (see Manam and Kaligatla [12])

$$g_j(u) = \frac{2}{\pi}u\sqrt{a^2-u^2}\int_0^a \frac{f_j'(t)}{\sqrt{a^2-t^2}(u^2-t^2)}dt,\ u\in(0,a)$$

provided that

$$\int_0^a \frac{f_j'(t)}{\sqrt{a^2-t^2}}dt = 0, \quad j=1,2,3. \tag{25}$$

The conditions (25) are expressed as

$$\lambda J_1(\lambda)C_1+\lambda_1J_1(\lambda_1)C_2+\bar\lambda_1J_1(\bar\lambda_1)C_3+\lambda_2J_1(\lambda_2)C_4+\bar\lambda_2J_1(\bar\lambda_2)C_5$$
$$-J_3(\lambda_2)D_1-J_3(\bar\lambda_2)D_2-\Big[\frac{\bar\lambda_1}{S(\bar\lambda_1)}J_1(-\bar\lambda_1)+\frac{i\bar\lambda_1}{S(\bar\lambda_1)}J_3(-\bar\lambda_1)\Big]A_2$$
$$-\alpha(\lambda_1)A_1-\alpha(\lambda)\eta_1-\Big[\frac{i\lambda}{S(\lambda)}J_3(-\lambda)+\frac{\lambda}{S(\lambda)}J_1(-\lambda)\Big]\eta_2=0, \qquad (26)$$

$$\lambda^3J_1(\lambda)C_1+\lambda_1^3J_1(\lambda_1)C_2+\bar\lambda_1^3J_1(\bar\lambda_1)C_3+\lambda_2^3J_1(\lambda_2)C_4+\bar\lambda_2^3J_1(\bar\lambda_2)C_5$$
$$-\lambda_2^2J_3(\lambda_2)D_1-\bar\lambda_2^2J_3(\bar\lambda_2)D_2-\Big[\frac{\bar\lambda_1^3}{S(\bar\lambda_1)}J_1(-\bar\lambda_1)+\frac{i\bar\lambda_1^3}{S(\bar\lambda_1)}J_3(-\bar\lambda_1)\Big]A_2$$
$$-\beta(\lambda_1)A_1-\beta(\lambda)\eta_1-\Big[\frac{i\lambda^3}{S(\lambda)}J_3(-\lambda)+\frac{\lambda^3}{S(\lambda)}J_1(-\lambda)\Big]\eta_2=0 \qquad (27)$$

and

$$\lambda^5J_1(\lambda)C_1+\lambda_1\bar\lambda_2^5J_1(\lambda_1)C_2+\bar\lambda_1^5J_1(\bar\lambda_1)C_3+\lambda_2^5J_1(\lambda_2)C_4+\bar\lambda_2^5J_1(\bar\lambda_2)C_5$$
$$-\lambda_2^4J_3(\lambda_2)D_1-\bar\lambda_2^4J_3(\bar\lambda_2)D_2-\Big[\frac{\bar\lambda_1^5}{S(\bar\lambda_1)}J_1(-\bar\lambda_1)+\frac{i\bar\lambda_1^5}{S(\bar\lambda_1)}J_3(-\bar\lambda_1)\Big]A_2$$
$$-\gamma(\lambda_1)A_1-\gamma(\lambda)\eta_1-\Big[\frac{i\lambda^5}{S(\lambda)}J_3(-\lambda)+\frac{\lambda^5}{S(\lambda)}J_1(-\lambda)\Big]\eta_2=0, \qquad (28)$$

where $\alpha(X)=\frac{X}{S(X)}J_1(-X)-\frac{iX}{S(X)}J_3(-X)$, $\beta(X)=\frac{X^3}{S(X)}J_1(-X)-\frac{iX^3}{S(X)}J_3(-X)$ and $\gamma(X)=\frac{X^5}{S(X)}J_1(-X)-\frac{iX^5}{S(X)}J_3(-X)$ with J_1,J_3 as in the Appendix. Finally, the conditions $g_1'(a)=h'(a)$ and $g_1'''(a)=h'''(a)$ may be modified as (see Manam and Kaligatla [12])

$$-ag_1'(a)=\int_0^a\frac{t^2f'''(t)}{\sqrt{a^2-t^2}}dt-\int_a^\infty\frac{t^2h''(t)}{\sqrt{t^2-a^2}}dt+\int_a^\infty th''(t)dt$$

and

$$-ag_1'''(a)=\int_0^a\frac{t^2f'''''(t)}{\sqrt{a^2-t^2}}dt-\int_a^\infty\frac{t^2h''''(t)}{\sqrt{t^2-a^2}}dt+\int_a^\infty th''''(t)dt.$$

These are further expressed as linear equations

$$\lambda^3J_2(\lambda)C_1+\lambda_1^3J_2(\lambda_1)C_2+\bar\lambda_1^3J_2(\bar\lambda_1)C_3+\lambda_2^3J_2(\lambda_2)C_4+\bar\lambda_2^3J_2(\bar\lambda_2)C_5$$

$$
\begin{aligned}
&+\Big[e^{\lambda_2 a}-\lambda_2^2 J_4(\lambda_2)\Big]D_1+\Big[e^{\bar\lambda_2 a}-\bar\lambda_2^2 J_4(\bar\lambda_2)\Big]D_2-\gamma_1(\lambda)\eta_1\\
&-\Big[\frac{i\lambda^3}{S(\lambda)}J_4(-\lambda)+\frac{\lambda^3}{S(\lambda)}J_2(-\lambda)-\frac{i\lambda}{S(\lambda)}e^{-\lambda a}\Big]\eta_2-\gamma_1(\lambda_1)A_1\\
&-\Big[\frac{\bar\lambda_1^3}{S(\bar\lambda_1)}J_2(-\bar\lambda_1)+\frac{i\bar\lambda_1^3}{S(\bar\lambda_1)}J_4(-\bar\lambda_1)-\frac{i\bar\lambda_1}{S(\bar\lambda_1)}e^{-\bar\lambda_1 a}\Big]A_2=0 \qquad (29)
\end{aligned}
$$

and

$$
\begin{aligned}
&\lambda^5 J_2(\lambda)C_1+\lambda_1\bar\lambda_2^5 J_2(\lambda_1)C_2+\bar\lambda_1^5 J_2(\bar\lambda_1)C_3+\lambda_2^5 J_2(\lambda_2)C_4+\bar\lambda_2^5 J_2(\bar\lambda_2)C_5\\
&\quad+\Big[\lambda_2^2 e^{\lambda_2 a}-\lambda_2^4 J_4(\lambda_2)\Big]D_1+\Big[\bar\lambda_2^2 e^{\bar\lambda_2 a}-\bar\lambda_2^4 J_4(\bar\lambda_2)\Big]D_2-\gamma_2(\lambda)\eta_1\\
&\quad-\Big[\frac{i\lambda^5}{S(\lambda)}J_4(-\lambda)+\frac{\lambda^5}{S(\lambda)}J_2(-\lambda)-\frac{i\lambda^3}{S(\lambda)}e^{-\lambda a}\Big]\eta_2-\gamma_2(\lambda_1)A_1\\
&\quad-\Big[\frac{\bar\lambda_1^5}{S(\bar\lambda_1)}J_2(-\bar\lambda_1)+\frac{i\bar\lambda_1^5}{S(\bar\lambda_1)}J_4(-\bar\lambda_1)-\frac{i\bar\lambda_1^3}{S(\bar\lambda_1)}e^{-\bar\lambda_1 a}\Big]A_2=0, \qquad (30)
\end{aligned}
$$

where $\gamma_1(X)=\frac{X^3}{S(X)}J_2(-X)-\frac{iX^3}{S(X)}J_4(-X)+\frac{iX}{S(X)}e^{-Xa}$ and $\gamma_2(X)=\frac{X^5}{S(X)}J_2(-X)-\frac{iX^5}{S(X)}J_4(-X)+\frac{iX^3}{S(X)}e^{-Xa}$ with J_2, J_4 as in the Appendix.

Then, the flexural gravity wave potentials $\psi_j, j=1,2$ are obtained as $\psi_1(x,y)=\chi(x,y)\ x>0, y>0$ with $\eta_1=R_1^1,\ \eta_2=R_2^1$ and $\psi_2(x,y)=\chi(-x,y)\ x<0, y>0$ with $\eta_1=R_2^2,\ \eta_2=R_1^2$.

By following the above solution procedure to the scattering problem involving the submerged vertical solid barrier, it is found that

$$
\begin{aligned}
\phi_j(x,y) &= (R-1)e^{i\lambda x-\lambda y}+B_1 e^{i\lambda_1 x-\lambda_1 y}+B_2 e^{-i\bar\lambda_1 x-\bar\lambda_1 y}\\
&\quad+\int_0^\infty B(\xi)\ L(\xi,y)\ e^{(-1)^j\xi x}\,d\xi, (-1)^{j+1}x>0, j=1,2,
\end{aligned}
$$

where $L(\xi,y)=\xi(1-M\xi^2+D\xi^4)\cos\xi y-K\sin\xi y$ and R, B_1, B_2, $B(\xi)$ are unknowns.

The function $B(\xi)$ will take the form of (20) with an appropriate $P(y)$ while the other constants satisfy the system of linear equations

$$
U_1+U_2+U_3+U_4+U_5+\frac{1}{S(\lambda)}R+\frac{1}{S(\lambda_1)}B_1+\frac{1}{S(\bar\lambda_1)}B_2=0, \qquad (31)
$$

$$
\lambda^2U_1+\lambda_1^2U_2+\bar\lambda_1^2U_3+\lambda_2^2U_4+\bar\lambda_2^2U_5+\frac{\lambda^2}{S(\lambda)}R+\frac{\lambda_1^2}{S(\lambda_1)}B_1+\frac{\bar\lambda_1^2}{S(\bar\lambda_1)}B_2=0, \qquad (32)
$$

$$\lambda^4 U_1 + \lambda_1^4 U_2 + \bar\lambda_1^4 U_3 + \lambda_2^4 U_4 + \bar\lambda_2^4 U_5 + \frac{\lambda^4}{S(\lambda)} R + \frac{\lambda_1^4}{S(\lambda_1)} B_1 + \frac{\bar\lambda_1^4}{S(\bar\lambda_1)} B_2 = 0, \quad (33)$$

$$\begin{aligned} e^{\lambda_2 a} V_1 + e^{\bar\lambda_2 a} V_2 - \frac{i\lambda}{S(\lambda)} e^{-\lambda a} R - \frac{i\lambda_1}{S(\lambda_1)} e^{-\lambda_1 a} B_1 + \frac{i\bar\lambda_1}{S(\bar\lambda_1)} e^{-\bar\lambda_1 a} B_2 & \\ = -\frac{i\lambda}{S(\lambda)} e^{-\lambda a}, & \quad (34) \end{aligned}$$

$$\begin{aligned} \lambda_2^2 e^{\lambda_2 a} V_1 + \bar\lambda_2^2 e^{\bar\lambda_2 a} V_2 - \frac{i\lambda^3}{S(\lambda)} e^{-\lambda a} R - \frac{i\lambda_1^3}{S(\lambda_1)} e^{-\lambda_1 a} B_1 + \frac{i\bar\lambda_1^3}{S(\bar\lambda_1)} e^{-\bar\lambda_1 a} B_2 & \\ = -\frac{i\lambda^3}{S(\lambda)} e^{-\lambda a}, & \quad (35) \end{aligned}$$

$$\begin{aligned} \lambda J_1(\lambda) U_1 + \lambda_1 J_1(\lambda_1) U_2 + \bar\lambda_1 J_1(\bar\lambda_1) U_3 + \lambda_2 J_1(\lambda_2) U_4 + \bar\lambda_2 J_1(\bar\lambda_2) U_5 & \\ - J_3(\lambda_2) V_1 - J_3(\bar\lambda_2) V_2 - \alpha(\lambda) R - \alpha(\lambda_1) B_1 & \\ - \Big[\frac{\bar\lambda_1}{S(\bar\lambda_1)} J_1(-\bar\lambda_1) + \frac{i\bar\lambda_1}{S(\bar\lambda_1)} J_3(-\bar\lambda_1) \Big] B_2 = \frac{i\lambda}{S(\lambda)} J_3(-\lambda), & \quad (36) \end{aligned}$$

$$\begin{aligned} \lambda^3 J_1(\lambda) U_1 + \lambda_1^3 J_1(\lambda_1) U_2 + \bar\lambda_1^3 J_1(\bar\lambda_1) U_3 + \lambda_2^3 J_1(\lambda_2) U_4 + \bar\lambda_2^3 J_1(\bar\lambda_2) U_5 & \\ - \lambda_2^2 J_3(\lambda_2) V_1 - \bar\lambda_2^2 J_3(\bar\lambda_2) V_2 - \beta(\lambda) R - \beta(\lambda_1) B_1 & \\ - \Big[\frac{\bar\lambda_1^3}{S(\bar\lambda_1)} J_1(-\bar\lambda_1) + \frac{i\bar\lambda_1^3}{S(\bar\lambda_1)} J_3(-\bar\lambda_1) \Big] B_2 = \frac{i\lambda^3}{S(\lambda)} J_3(-\lambda), & \quad (37) \end{aligned}$$

$$\begin{aligned} \lambda^5 J_1(\lambda) U_1 + \lambda_1 \bar\lambda_2^5 J_1(\lambda_1) U_2 + \bar\lambda_1^5 J_1(\bar\lambda_1) U_3 + \lambda_2^5 J_1(\lambda_2) U_4 + \bar\lambda_2^5 J_1(\bar\lambda_2) U_5 & \\ - \lambda_2^4 J_3(\lambda_2) V_1 - \bar\lambda_2^4 J_3(\bar\lambda_2) V_2 - \gamma(\lambda) R - \gamma(\lambda_1) B_1 & \\ - \Big[\frac{\bar\lambda_1^5}{S(\bar\lambda_1)} J_1(-\bar\lambda_1) + \frac{i\bar\lambda_1^5}{S(\bar\lambda_1)} J_3(-\bar\lambda_1) \Big] B_2 = \frac{i\lambda^5}{S(\lambda)} J_3(-\lambda), & \quad (38) \end{aligned}$$

$$\lambda^3 J_2(\lambda)U_1 + \lambda_1^3 J_2(\lambda_1)U_2 + \bar{\lambda}_1^3 J_2(\bar{\lambda}_1)U_3 + \lambda_2^3 J_2(\lambda_2)U_4 + \bar{\lambda}_2^3 J_2(\bar{\lambda}_2)U_5$$
$$+\Big[e^{\lambda_2 a} - \lambda_2^2 J_4(\lambda_2)\Big]V_1 + \Big[e^{\bar{\lambda}_2 a} - \bar{\lambda}_2^2 J_4(\bar{\lambda}_2)\Big]V_2 - \gamma_1(\lambda)R - \gamma_1(\lambda_1)B_1$$
$$-\Big[\frac{\bar{\lambda}_1^3}{S(\bar{\lambda}_1)}J_2(-\bar{\lambda}_1) + \frac{i\bar{\lambda}_1^3}{S(\bar{\lambda}_1)}J_4(-\bar{\lambda}_1) - \frac{i\bar{\lambda}_1}{S(\bar{\lambda}_1)}e^{-\bar{\lambda}_1 a}\Big]B_2$$
$$= \frac{i\lambda^3}{S(\lambda)}J_4(-\lambda) - \frac{i\lambda}{S(\lambda)}e^{-\lambda a}, \quad (39)$$

and

$$\lambda^5 J_2(\lambda)U_1 + \lambda_1^5 J_2(\lambda_1)U_2 + \bar{\lambda}_1^5 J_2(\bar{\lambda}_1)U_3 + \lambda_2^5 J_2(\lambda_2)U_4 + \bar{\lambda}_2^5 J_2(\bar{\lambda}_2)U_5$$
$$+\Big[\lambda_2^2 e^{\lambda_2 a} - \lambda_2^4 J_4(\lambda_2)\Big]V_1 + \Big[\bar{\lambda}_2^2 e^{\bar{\lambda}_2 a} - \bar{\lambda}_2^4 J_4(\bar{\lambda}_2)\Big]V_2 - \gamma_2(\lambda)R - \gamma_2(\lambda_1)B_1$$
$$-\Big[\frac{\bar{\lambda}_1^5}{S(\bar{\lambda}_1)}J_2(-\bar{\lambda}_1) + \frac{i\bar{\lambda}_1^5}{S(\bar{\lambda}_1)}J_4(-\bar{\lambda}_1) - \frac{i\bar{\lambda}_1^3}{S(\bar{\lambda}_1)}e^{-\bar{\lambda}_1 a}\Big]B_2$$
$$= \frac{i\lambda^5}{S(\lambda)}J_4(-\lambda) - \frac{i\lambda^3}{S(\lambda)}e^{-\lambda a}, \quad (40)$$

where $U_j, j = 1, 2, 3, 4, 5$ and $V_j, j = 1, 2$ are unknown constants.

Now, by using far-field behavior of the each term in the connection (10), it may be obtained that

$$(1 + \Gamma)R_p = R + R_1^1, \quad (41)$$
$$\Gamma R_p = -R_2^1 \quad (42)$$

for $j = 1$ and

$$(1 + \Gamma)R_p = R + R_2^2, \quad (43)$$
$$\Gamma R_p = -R_1^2 \quad (44)$$

for $j = 2$.
The linear equations (17)-(19), (23)-(24) and (26)-(40) with $\eta_1 = R_1^1$, $\eta_2 = R_2^1$ or $\eta_1 = R_2^2$, $\eta_2 = R_1^2$ along with (41)-(42) or (43)-(44), respectively, are solved to find all the unknown constants involved in the problem. Thus, the porous potentials $\phi_j^p(x, y), j = 1, 2$ are explicitly known from the relation (13).

2.2.2. capillary or membrane-coupled gravity wave scattering

The general problem for $\chi(x,y), x>0, y>0$ in this case is (1), (2) with $D=0$, (5), (11)-(12) and (14). $\chi(x,y)$ is routinely determined as (see Manam [10])

$$\chi(x,y)=\eta_1 e^{i\lambda x-\lambda y}+\eta_2 e^{-i\lambda x-\lambda y}+\int_0^\infty A(\xi)\ L_1(\xi,y)\ e^{-\xi x}\,d\xi,\quad x>0, y>0,$$

where $L_1(\xi,y)=\xi(1-M\xi^2)\cos\xi y-K\sin\xi y$, η_1, η_2, and $A(\xi)$ are unknowns. Also, λ is a positive real root of the dispersion equation $Mx^3+x-K=0$. The equation has complex conjugate roots $\lambda_1, \bar{\lambda}_1$ with a negative real part. Then, the unknowns involved are found to satisfy the linear equations

$$C_1+C_2+C_3+\frac{1}{S_1(\lambda)}\eta_1+\frac{1}{S_1(\lambda)}\eta_2=0, \tag{45}$$

$$\lambda^2 C_1+\lambda_1^2 C_2+\bar{\lambda}_1^2 C_3+\frac{\lambda^2}{S_1(\lambda)}\eta_1+\frac{\lambda^2}{S_1(\lambda)}\eta_2=0, \tag{46}$$

$$e^{\lambda_1 a}D_1+e^{\bar{\lambda}_1 a}D_2-\frac{i\lambda}{S_1(\lambda)}e^{-\lambda a}\eta_1+\frac{i\lambda}{S_1(\lambda)}e^{-\lambda a}\eta_2=0, \tag{47}$$

$$\begin{aligned}\lambda J_1(\lambda)C_1+\lambda_1 J_1(\lambda_1)C_2+\bar{\lambda}_1 J_1(\bar{\lambda}_1)C_3-J_3(\lambda_1)D_1-J_3(\bar{\lambda}_1)D_2&\\ -\alpha(\lambda)\eta_1-\Big[\frac{i\lambda}{S_1(\lambda)}J_3(-\lambda)+\frac{\lambda}{S_1(\lambda)}J_1(-\lambda)\Big]\eta_2=0,&\end{aligned} \tag{48}$$

$$\begin{aligned}\lambda^3 J_1(\lambda)C_1+\lambda_1^3 J_1(\lambda_1)C_2+\bar{\lambda}_1^3 J_1(\bar{\lambda}_1)C_3-\lambda_1^2 J_3(\lambda_1)D_1-\bar{\lambda}_1^2 J_3(\bar{\lambda}_1)D_2&\\ -\beta(\lambda)\eta_1-\Big[\frac{i\lambda^3}{S_1(\lambda)}J_3(-\lambda)+\frac{\lambda^3}{S_1(\lambda)}J_1(-\lambda)\Big]\eta_2=0,&\end{aligned} \tag{49}$$

$$\begin{aligned}\lambda^3 J_2(\lambda)C_1+\lambda_1^3 J_2(\lambda_1)C_2+\bar{\lambda}_1^3 J_2(\bar{\lambda}_1)C_3+\Big[e^{\lambda_1 a}-\lambda_1^2 J_4(\lambda_1)\Big]D_1&\\ +\Big[e^{\bar{\lambda}_1 a}-\bar{\lambda}_1^2 J_4(\bar{\lambda}_1)\Big]D_2-\gamma(\lambda)\eta_1-\Big[\frac{i\lambda^3}{S_1(\lambda)}J_4(-\lambda)+\frac{\lambda^3}{S_1(\lambda)}J_2(-\lambda)\Big]\eta_2=0,&\end{aligned} \tag{50}$$

where $S_1(X)=X(1+MX^2)+K$, $\alpha(\lambda)=\frac{\lambda}{S_1(\lambda)}J_1(-\lambda)-\frac{i\lambda}{S_1(\lambda)}J_3(-\lambda)$, $\beta(\lambda)=\frac{\lambda^3}{S_1(\lambda)}J_1(-\lambda)-\frac{i\lambda^3}{S_1(\lambda)}J_3(-\lambda)$, $\gamma(\lambda)=\frac{\lambda^3}{S_1(\lambda)}J_2(-\lambda)-\frac{i\lambda^3}{S_1(\lambda)}J_4(-\lambda)+\frac{i\lambda}{S_1(\lambda)}e^{-\lambda a}$ and C_j, D_j are arbitrary constants.

Then, the membrane-coupled gravity wave potentials $\psi_j, j = 1, 2$ are obtained as $\psi_1(x, y) = \chi(x, y)\ x > 0, y > 0$ with $\eta_1 = R_1^1,\ \eta_2 = R_2^1$ and $\psi_2(x, y) = \chi(-x, y)\ x < 0, y > 0$ with $\eta_1 = R_2^2,\ \eta_2 = R_1^2$.

The solid wave potentials $\phi_j, j = 1, 2$ are similarly obtained as

$$\phi_j(x, y) = (R-1)e^{i\lambda x-\lambda y} + \int_0^\infty B(\xi)\ L_1(\xi, y)\ e^{(-1)^j\xi x}\, d\xi, (-1)^{j+1}x > 0, j = 1, 2,$$

where $L_1(\xi, y) = \xi(1 - M\xi^2)\cos\xi y - K\sin\xi y$ and R, $B(\xi)$ are unknowns. Again, The function $B(\xi)$ takes the form of (20) with appropriate $P(y)$ while the reflection amplitude R satisfies the system of linear equations

$$U_1 + U_2 + U_3 + \frac{1}{S_1(\lambda)}R = 0, \tag{51}$$

$$\lambda^2 U_1 + \lambda_1^2 U_2 + \bar{\lambda}_1^2 U_3 + \frac{\lambda^2}{S_1(\lambda)}R = 0, \tag{52}$$

$$e^{\lambda_1 a}V_1 + e^{\bar{\lambda}_1 a}V_2 - \frac{i\lambda}{S_1(\lambda)}e^{-\lambda a}R = -\frac{i\lambda}{S_1(\lambda)}e^{-\lambda a}, \tag{53}$$

$$\begin{aligned}\lambda J_1(\lambda)U_1 + \lambda_1 J_1(\lambda_1)U_2 + \bar{\lambda}_1 J_1(\bar{\lambda}_1)U_3 - J_3(\lambda_1)V_1 - J_3(\bar{\lambda}_1)V_2 \\ -\alpha(\lambda)R = \frac{i\lambda}{S_1(\lambda)}J_3(-\lambda),\end{aligned} \tag{54}$$

$$\begin{aligned}\lambda^3 J_1(\lambda)U_1 + \lambda_1^3 J_1(\lambda_1)U_2 + \bar{\lambda}_1^3 J_1(\bar{\lambda}_1)U_3 - \lambda_1^2 J_3(\lambda_1)V_1 - \bar{\lambda}_1^2 J_3(\bar{\lambda}_1)V_2 \\ -\beta(\lambda)R = \frac{i\lambda^3}{S_1(\lambda)}J_3(-\lambda),\end{aligned} \tag{55}$$

and

$$\begin{aligned}\lambda^3 J_2(\lambda)U_1 + \lambda_1^3 J_2(\lambda_1)U_2 + \bar{\lambda}_1^3 J_2(\bar{\lambda}_1)U_3 + \left[e^{\lambda_1 a} - \lambda_1^2 J_4(\lambda_1)\right]V_1 \\ +\left[e^{\bar{\lambda}_1 a} - \bar{\lambda}_1^2 J_4(\bar{\lambda}_1)\right]V_2 - \gamma(\lambda)R = \frac{i\lambda^3}{S_1(\lambda)}J_4(-\lambda) - \frac{i\lambda}{S_1(\lambda)}e^{-\lambda a},\end{aligned} \tag{56}$$

where $U_j, j = 1, 2, 3$ and $V_j, j = 1, 2$ are constants.

The system of equations (51)-(56) will determine the reflection amplitude R of the submerged solid barrier while (45)-(50) with $\eta_1 = R_1^1,\ \eta_2 = R_2^1$ or $\eta_1 = R_2^2,\ \eta_2 = R_1^2$ along with relations (41)-(42) or (43)-(44), respectively, produce the reflection amplitude R_p and the other unknowns in an explicit form.

3. Mathematical problem and its solution approach for surface piercing porous barrier case

We consider the scattering problem involving a surface piercing barrier when the surface is covered with either a membrane or surface tension by assuming $D = 0$ in (2). In the former case, both side of the barriers, membrane is connected with a spring of zero stiffness (see Manam [10]). Then, the spatial potentials $\hat{\phi}_j(x,y), j = 1,2$ satisfy the mixed boundary value problem $(1) - (7)$ with $B = (0,a)$ and $G = (a,\infty)$.
It may be observed, due to the surface tension effect, the horizontal velocity of the fluid is not continuous at the piercing point $(0,0)$. In order to make the problem in which horizontal velocity is continuous across $x = 0$ and to utilize the previously established solution procedure, we define a new potential as given by

$$\sigma_j(x,y) = \hat{\phi}_j(x,y) - \hat{\phi}^c_j(x,y), \ -\infty < x < \infty, y > 0, j = 1,2. \tag{57}$$

In the above, ϕ^c_j is the complex potential associated with wave scattering by complete porous wall occupying the position at $x = 0, y > 0$. Then, $\phi^c_j,\ j = 1,2$ may be obtained (see Manam et al. [11]) as

$$\hat{\phi}^c_j(x,y) = \begin{cases} \phi^0(-x,y) + R_c\ \phi^0(x,y) + \displaystyle\int_0^\infty E_1(\xi)L_1(\xi,y)e^{-\xi|x|}\,d\xi,\ (-1)^{j+1}x > 0, \\ T_c\ \phi^0(-x,y) + \displaystyle\int_0^\infty E_2(\xi)L_1(\xi,y)e^{-\xi|x|}\,d\xi,\ (-1)^{j+1}x < 0, \end{cases}$$

where λ is the positive real root of the dispersion equation $Mx^3 + x - K = 0$ and $L_1(\xi,y) = \xi(1 - M\xi^2)\cos\xi y - K\sin\xi y$. Also, in the above, by utilizing the mode-coupling relation on orthogonal functions $L_1(\xi,y)$ and $e^{-\lambda y}$ (see Manam [10]), the reflection and transmission amplitudes of the incident wave from the complete porous barrier are obtained in an explicit form as given by

$$R_c = 1 - T_c + \frac{2iM(\mu^- - \mu^+)}{(1 + 3M\lambda^2)} = \frac{1}{1 + 2\Gamma}\Big[1 + 2iM\Gamma\frac{(\mu^- - \mu^+)}{(1 + 3M\lambda^2)}\Big],$$
$$E_1(\xi) = -E_2(\xi) + \frac{M(\mu^- - \mu^+)}{\Delta(\xi)} = -i\lambda M\Gamma\frac{(\mu^- - \mu^+)}{\Delta(\xi)(\xi - 2i\lambda\Gamma)},$$

where $\mu^\pm = \dfrac{\partial\hat{\phi}^c_j(0\pm,0)}{\partial x\partial y}$ are undetermined constants in the problem and $\Delta(\xi) = \xi^2(1 - M\xi^2)^2 + K^2$.

Also, first it may be observed that if $((\hat{\phi}_j)_x(0-,0) - (\hat{\phi}_j)_x(0+,0)) = ((\hat{\phi}^c_j)_x(0-,0) - (\hat{\phi}^c_j)_x(0+,0))$, then $((\hat{\phi}_j)_x(0-,y) - (\hat{\phi}_j)_x(0+,y)) = ((\hat{\phi}^c_j)_x(0^-,y) - (\hat{\phi}^c_j)_x(0+,y))$ for all $y > 0$ and subsequently, the potential $\frac{\partial \sigma_j}{\partial x}$ is continuous across $x = 0$. Then the undetermined constant $(\mu^- - \mu^+)$ will carry forward to the problem for $\sigma_j(x,y)$ since $(\mu^- - \mu^+) = \Big(\frac{\partial \hat{\phi}_j(0-,0)}{\partial x \partial y} - \frac{\partial \hat{\phi}_j(0+,0)}{\partial x \partial y}\Big)$. In other words, the undetermined constant $(\mu^- - \mu^+)$ in the scattering problem involving the complete porous barrier has been fed from the last equality. Since the membrane cover is connected to the barriers with the spring of zero stiffness, then $\frac{\partial \hat{\phi}_j(0-,0)}{\partial x \partial y} = \frac{\partial \hat{\phi}_j(0+,0)}{\partial x \partial y} = 0$. In the case of free surface with surface tension these constants, $\frac{\partial \hat{\phi}_j(0-,0)}{\partial x \partial y}$, $\frac{\partial \hat{\phi}_j(0+,0)}{\partial x \partial y}$ are also known as edge slope constants at the surface. (see Manam [10])

Now, the partial derivatives ${\sigma_j}_x, j = 1,2$ are continuous at $x = 0, \forall y \geq 0$. It is clear from the definition (57) that the potentials $\sigma_j, j = 1,2$ satisfy (1)-(3), (5)and (7) . The new potentials $\sigma_j(x,y), j = 1,2$ can be decomposed as (see Lamb [7])

$$\sigma_j(x,y) = \begin{cases} \varphi_j(x,y), & (-1)^{j+1}x > 0, \\ -\varphi_j(-x,y), & (-1)^{j+1}x < 0. \end{cases}$$

The functions $\varphi_j(x,y), j = 1,2$ defined in the quarter plane satisfy (1)-(2), (5) and (7) along with

$$\begin{aligned} &\varphi_{j_x}(0,y) + 2i\lambda\Gamma\varphi_j(0,y) = 0,\ y \in (0,a), \\ &\varphi_j(0,y) = q_j(y),\ y \in (a,\infty), \\ &\varphi_j(x,y) \sim\ (R_p - R_c)\phi^0(x,y),\ x \to \infty, \end{aligned}$$

where the function $q_j(y), j = 1,2$ is given by

$$\begin{aligned} q_j(y) &= \frac{1}{2}(-1)^j(\phi^c_j(0+,y) - \phi^c_j(0-,y)),\ y \in (a,\infty), \\ &= R_q e^{-\lambda y} + \int_0^\infty E(\xi)L_1(\xi,y)\,d\xi,\ y \in (a,\infty) \end{aligned}$$

with

$$R_q = \frac{1}{1+2\Gamma}\Big(\frac{iM(\mu^- - \mu^+)}{1+3M\lambda^2} - 1\Big),\ E(\xi) = \frac{M}{2}\frac{\xi(\mu^- - \mu^+)}{\Delta(\xi)(\xi - 2i\lambda\Gamma)}.$$

Next, the above quarter plane problems for the solution potentials $\varphi_j(x,y), j = 1,2$ are solved by defining a connection between them and a relatively easily obtainable potentials, also known as auxiliary potentials.

3.1. Determination of the potentials

The connection between the solution and the auxiliary potentials may be defined as

$$\begin{aligned}\varphi_j(x,y) + i\lambda\Gamma\int_0^x \Big[\varphi_1((-1)^{j+1}t,y) + \varphi_2((-1)^j t,y)\Big]\,dt \\ = \Omega_j(x,y), (-1)^{j+1}x > 0, j = 1,2,\end{aligned}$$

where the auxiliary potential Ω_j satisfies (1)-(2) and (5). Then, it can be easily verified that the potential $\Omega_j, j = 1,2$, satisfies the boundary conditions

$$\Omega_{j_x}(0,y) = 0,\ y \in (0,a), \tag{58}$$
$$\Omega_j(0,y) = q_j(y),\ y \in (a,\infty), \tag{59}$$
$$\Omega_j(x,y) \sim R_{1j}\phi^0(x,y) + R_{2j}\phi^0(-x,y),\ (-1)^{j+1}x \to \infty, \tag{60}$$

where the $R_{1j}, R_{2j},\ j = 1,2$ are unknown constants such that

$$R_{11} - R_{21} = (1+2\Gamma)(R_p - R_c),\ R_{11} + R_{21} = R_p - R_c, \tag{61}$$

and

$$R_{22} - R_{12} = (1+2\Gamma)(R_p - R_c),\ R_{22} + R_{12} = R_p - R_c. \tag{62}$$

The potential function $\Omega(x,y)$ that satisfies (1)-(2),(5) and (60) may be expanded as

$$\Omega(x,y) = R_1 e^{i\lambda x - \lambda y} + R_2 e^{-i\lambda x - \lambda y} + \int_0^\infty C(\xi)L_1(\xi,y)e^{-\xi x}\,d\xi, x > 0, y > 0.$$

where R_1, R_2, $C(\xi)$ are the unknowns and λ_1 and $\bar{\lambda_1}$ are the other two roots of dispersion relation. It is seen that $\Omega_1(x,y) = \Omega(x,y),\ x > 0$ with $R_1 = R_{11}$, $R_2 = R_{21}$ and $\Omega_2(x,y) = \Omega(-x,y),\ x > 0$ with $R_1 = R_{22}$, $R_2 = R_{12}$.

A pair of integral equations are obtained by using the boundary conditions (58) and (59). These integral equations are solved by the procedure as in Manam [10], Manam and Kaligatla [12]. Then the unknowns R_1 and R_2 satisfy a system of linear equations

$$G_1 + G_2 + G_3 - \frac{i\lambda}{S_1(\lambda)}(R_1 - R_2) = 0, \tag{63}$$

$$G_1\lambda^2 + G_2\lambda_1^2 + G_3\bar{\lambda}_1^2 - \frac{i\lambda^3}{S_1(\lambda)}(R_1 - R_2) = 0, \tag{64}$$

$$G_1e^{\lambda a} + G_2e^{\lambda_1 a} + G_3e^{\bar{\lambda}_1 a} - \frac{i\lambda}{S_1(\lambda)}(R_1 - R_2)e^{-\lambda a} = 0, \tag{65}$$

$$\begin{aligned} &J_5(\lambda)G_1 + J_5(\lambda_1)G_2 + J_5(\bar{\lambda_1})G_3 + \lambda_1 J_6(\lambda_1)F_1 + \bar{\lambda_1}J_6(\bar{\lambda_1})F_2 \\ &-\frac{\lambda}{S_1(\lambda)}J_6(-\lambda)(R_1 + R_2 - R_q) - \frac{i\lambda}{S_1(\lambda)}J_5(-\lambda)(R_1 - R_2) \\ &= -\int_a^\infty \int_0^\infty \frac{t\ \xi E(\xi)\cos\xi t}{\sqrt{t^2 - a^2}} d\xi dt, \end{aligned} \tag{66}$$

$$\begin{aligned} &\lambda^2 J_5(\lambda)G_1 + \lambda_1^2 J_5(\lambda_1)G_2 + \bar{\lambda_1}^2 J_5(\bar{\lambda_1})G_3 + \lambda_1^3 J_6(\lambda_1)F_1 + \bar{\lambda_1}^3 J_6(\bar{\lambda_1})F_2 \\ &-\frac{\lambda^3}{S_1(\lambda)}J_6(-\lambda)(R_1 + R_2 - R_q) - \frac{i\lambda^3}{S_1(\lambda)}J_5(-\lambda)(R_1 - R_2) \\ &= \int_a^\infty \int_0^\infty \frac{t\ \xi^3 E(\xi)\cos\xi t}{\sqrt{t^2 - a^2}} d\xi dt, \end{aligned} \tag{67}$$

$$\begin{aligned} &\lambda J_1(\lambda)G_1 + \lambda_1 J_1(\lambda_1)G_2 + \bar{\lambda_1}J_1(\bar{\lambda_1})G_3 + \lambda_1^2 J_3(\lambda_1)F_1 + \bar{\lambda_1}^2 J_3(\bar{\lambda_1})F_2 \\ &+\frac{\lambda^2}{S_1(\lambda)}J_3(-\lambda)(R_1 + R_2 - R_q) + \frac{i\lambda^2}{S_1(\lambda)}J_1(-\lambda)(R_1 - R_2) \\ &= \int_a^\infty \int_0^\infty \frac{\xi^2 E(\xi)\sin\xi t}{\sqrt{t^2 - a^2}} d\xi dt, \end{aligned} \tag{68}$$

where J_1, J_3, J_5 and J_6 are given in the Appendix.

These set of six equations (63)-(68) and a pair of equations in (61) or (62) are solved by taking either $R_1 = R_{11}$,$R_2 = R_{21}$ or $R_1 = R_{22}$,$R_2 = R_{12}$ for the eight unknown coefficients $G_1, G_2, G_3, F_1, F_2, R_1, R_2$ and R_p interms of $\mu^- - \mu^+$.

4. Numerical results

4.1. Flexural or ice-coupled gravity waves with submerged barrier

Numerical results are evaluated for the reflection coefficient and the total energy against a wave parameter. Conservation of energy $|R_p|^2 + |T_p|^2 = 1$

is validated when $\Gamma = 0$ for two barrier positions. In the computation, parameters Young modulus $E = 5GPa$, Poisson's ratio $\nu = 0.3$, ice density $\rho_i = 922.5\ kg\ m^{-3}$, water density $\rho = 1025.0\ kg\ m^{-3}$, acceleration due to gravity $g = 9.81\ ms^{-2}$ are fixed. A typical value $\tau = -(EI\rho g)^{1/2}$ is chosen for the compressive force on the floating structure.

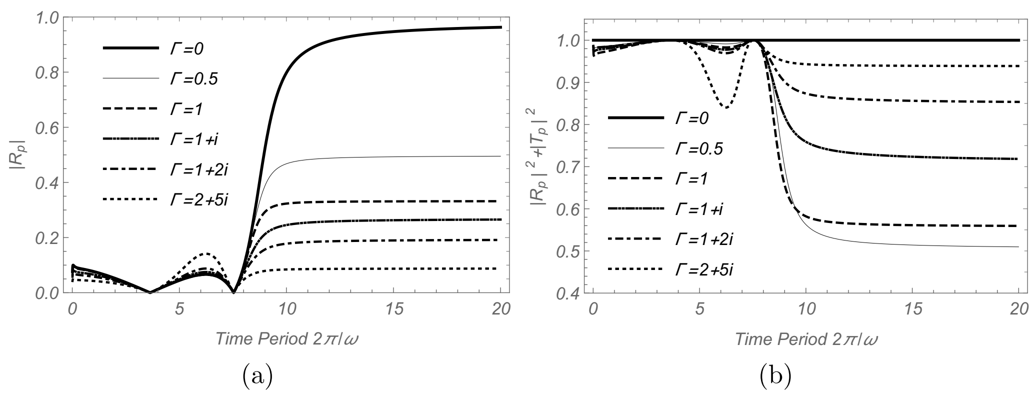

Figure 1: Variation of (a) reflection coefficient and (b) total wave energy against time period $2\pi/\omega$ when $d = 0.5m$ and $a = 1m$.

In Figures 1–2, the reflection coefficient and the total energy for flexural gravity waves are plotted against the time period $T = 2\pi/\omega$ for different values of the porous parameter Γ when the thickness of the compressed plate $d = 0.5m$ and the submerged depths $a = 1m, 20m$ respectively are kept fixed. As observed in Manam and Kaligatla [12], enhanced reflection at certain smaller time periods is sensitive to both the depth of submergence and the plate thickness. For waves with these shorter time periods, reflection as well as energy dissipation is found to be significantly small for any porous parameter. At certain short to moderate resonant time periods of the incident wave, significant energy dissipation is caused by the porous barrier. For waves with moderate to longer time periods, 40-50% of the wave energy is dissipated and 9-20% of the energy is reflected by the barrier when the the porous barrier is considered with resistant effects in the moderate range $\Gamma = 0.5$ to 1.0. Also, flexural gravity waves with certain time periods pass through the porous barrier completely without any dissipation of energy. The time period of these fully transmitted waves becomes longer with an increase in the submerged depth of the barrier.

Figure 3 depicts that flexural gravity waves with small and intermediate

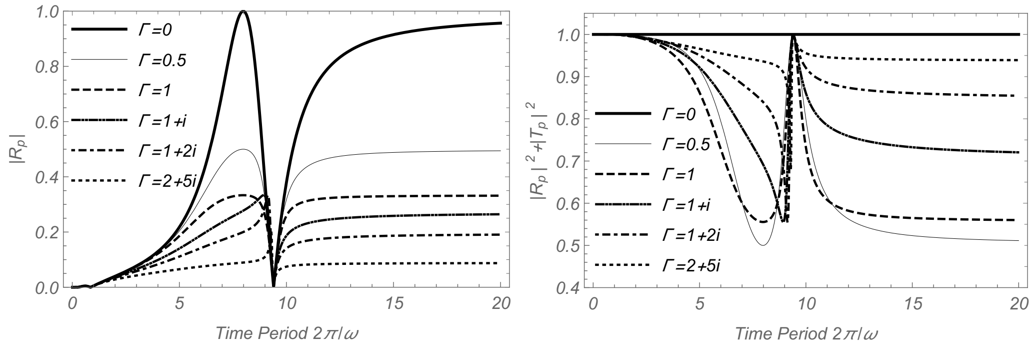

(a) (b)

Figure 2: Variation of (a) reflection coefficient and (b) total wave energy against time period $2\pi/\omega$ when $d = 0.5m$ and $a = 20m$.

time periods have higher reflection than the flexural gravity waves under the compressive force while those with longer time periods have slightly lower reflection.

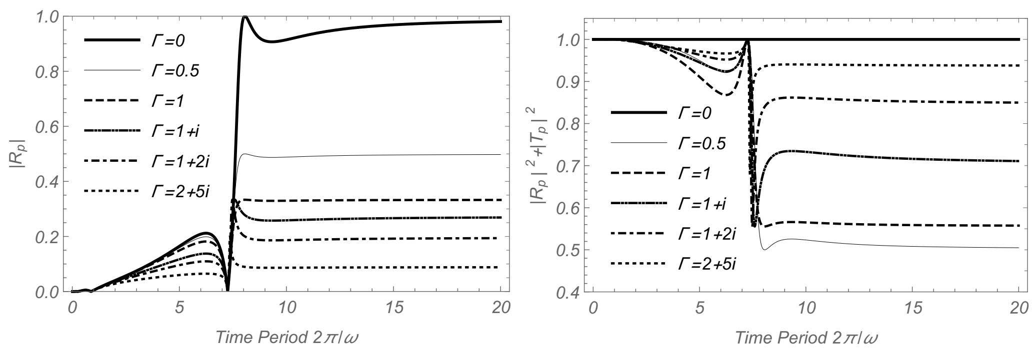

(a) (b)

Figure 3: Variation of (a) reflection coefficient and (b) total wave energy against time period $2\pi/\omega$ when $d = 0.5m$, $a = 20m$ and $\tau = 0$.

4.2. Capillary or membrane-coupled gravity waves with submerged barrier

The reflection coefficient and the total energy are plotted against the non-dimensional wave parameter Ka for different values of the non-dimensional membrane tension parameter $\beta = MK^2$. A typical value of β chosen for water at the room temperature is 0.074. The reflection and the energy curves for capillary gravity waves in this case are shown in Figure 4. Enhanced reflection as well as significant energy dissipation takes place at certain frequencies which is due to the interplay between the surface tension and the incident wave frequencies for all Γ values. However, moderate values of resistance effects in the porous parameter Γ cause significant enhancement in the reflection and dissipation as compared to the inertial effects in Γ. Figure 5 shows similar results for membrane coupled gravity waves with widening the gap between resonant frequencies. Clearly, surface or membrane tension causes enhanced reflection and porosity causes energy dissipation significantly at the resonant frequencies.

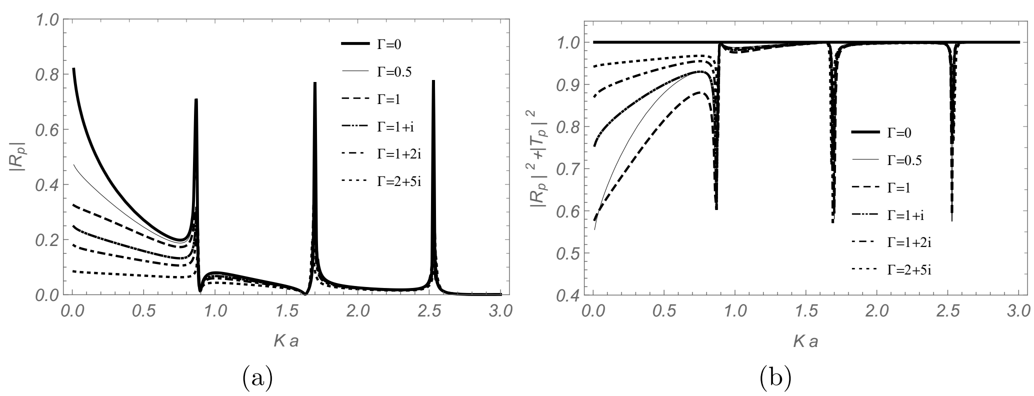

Figure 4: Variation of (a) reflection coefficient and (b) total wave energy against the non-dimensional wavenumber Ka when $\beta = 0.074$.

4.3. Capillary or membrane-coupled gravity waves with surface piercing barrier

The coefficient of reflection and total energy are evaluated against the time period and non-dimensional wavenumber for membrane-coupled gravity waves incident on the surface piercing barrier. Computations have been done for the same edge slope constants. In Figure 6, reflection and energy curves are depicted versus time period when $\beta = 0.1$ and $a = 1m$. Figure 6, shows that reflection decreases as absolute value of porous effect parameter Γ increases and energy loss increases as absolute value of non-zero Γ value increases for waves with smaller time periods. Reflection of a solid barrier is expectedly high. In Figures 7–8, reflection and energy curves are plotted against the wavenumber Ka for various porous effect parameter Γ values

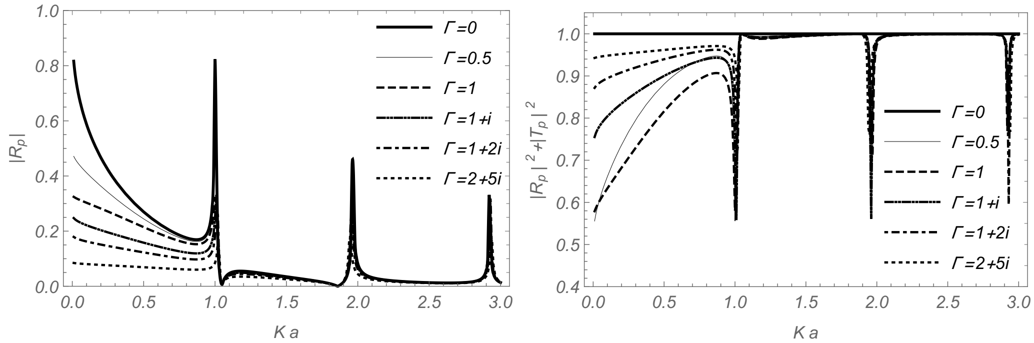

(a) (b)

Figure 5: Variation of (a) reflection coefficient and (b) total wave energy against the non-dimensional wavenumber Ka when $\beta = 0.1$.

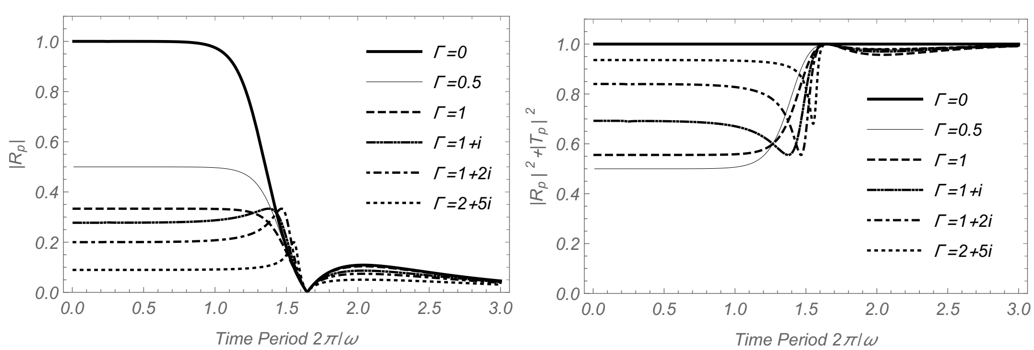

(a) (b)

Figure 6: Variation of (a) reflection coefficient and (b) total wave energy against the against time period $2\pi/\omega$ when $\beta = 0.1$ and $a = 1m$.

with parameter values $\beta = 0.074$ and $\beta = 0.1$, respectively. The former one for water with surface tension and latter for a tensioned membrane. Figures 7–8 depict that reflection increases with the decrease in the inertial and the resistance of the porous parameter for all wavenumbers. Complete transmission occurs for waves with certain frequencies. Moreover, dissipation of wave energy is mostly caused by the resistance effect of the porous parameter and this happens for moderate to higher wavenumbers.

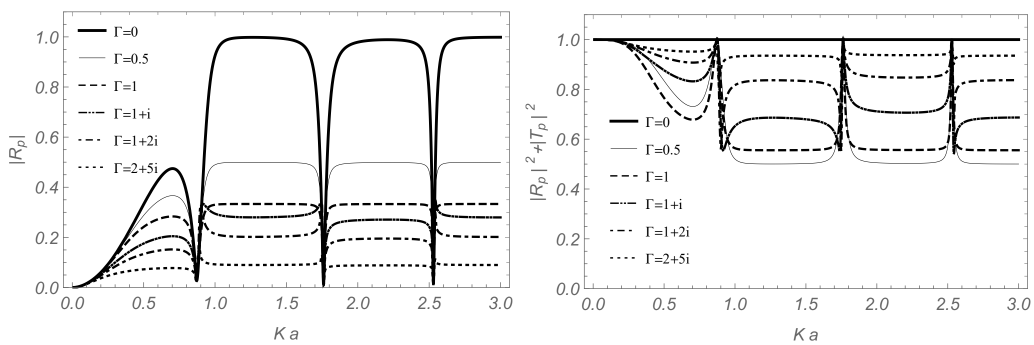

(a) (b)

Figure 7: Variation of (a) reflection coefficient and (b) total wave energy against the non-dimensional wavenumber Ka when $\beta = 0.074$.

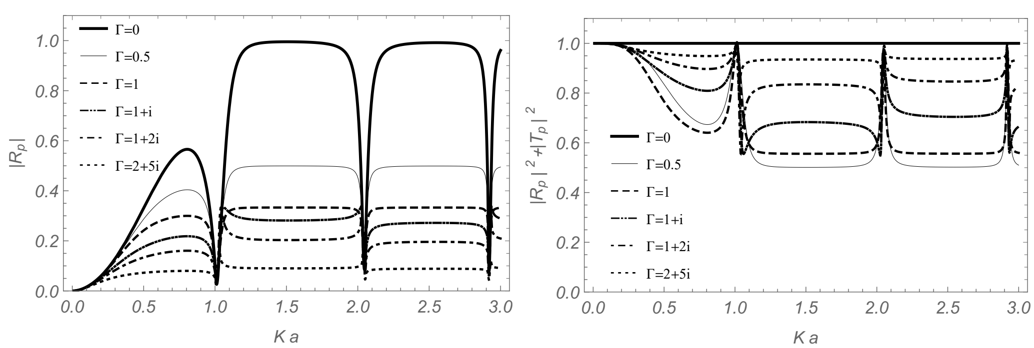

(a) (b)

Figure 8: Variation of (a) reflection coefficient and (b) total wave energy against the non-dimensional wavenumber Ka when $\beta = 0.1$.

5. Conclusions

Structure-coupled gravity wave scattering by a submerged vertical porous barrier is explicitly solved by utilizing a connection between its solution wave potential and the one pertaining to wave scattering by a submerged vertical solid barrier. Also membrane coupled wave scattering by a surface piercing porous barrier is explicitly solved by a similar connection between the wave potentials. The method decomposes the original problem into two explicitly solvable ones. Then, by solving the involved integral connections, the solution wave potentials of the original problems are explicitly determined.

Numerical results for the explicitly found scattering quantities are graphically presented. It is found that porous barriers with moderate resistance effects cause much desirable wave reflection and energy dissipation. At certain resonant frequencies, enhanced reflection is caused by the membrane tension while significant energy dissipation is caused by the porous barrier. Further, complete transmission of capillary or membrane-coupled gravity waves past the surface piercing porous barrier occurs at certain resonant wave frequencies.

Acknowledgements

The work is supported by DST with grant no. MTR/2019/000561.

References

1. H. Behera, T. Sahoo and C. O. Ng, Effect of a Submerged Porous Plate on the Hydroelastic Response of a Very Large Floating Structure, *J. Marine Sci. Appl.*, **17**(2018), 564–577.

2. D. Das and B. N. Mandal, Oblique wave scattering by a circular cylinder submerged beneath an ice-cover, *Int. Jl. Engrg. Sci.*, **44**(2006), 166–179.

3. D. Das and B. N. Mandal, Wave scattering by a circular cylinder half-immersed in water with an ice-cover, *Int. Jl. Engrg. Sci.*, **47**(2009), 463–474.

4. C. Fox and V.A. Squire, Reflection and transmission characteristics at the edge of shore fast sea ice, *Jl. Geophys. Res.*, **95**(1990), 611–629.

5. D. Karmakar, J. Bhattacharjee and T. Sahoo, Wave interaction with multiple articulated floating elastic plates, *Journal of Fluids and Structures*, **25**(2009), 1065–1078.

6. N. S. Karp and C. F. Karal, The elastic field behaviour in the neighbourhood of a crack of arbitrary angle, *Commn. Pure and Appl. Math.*, **15**(1962), 413–421.

7. H. Lamb, *Hydrodynamics*,Cambridge University Press, Cambridge, 1932.

8. C. M. Linton and H. Chung, Reflection and transmission at the ocean/sea-ice boundary, *Wave Motion*, **1126**(2003), 1–10.

9. P. Maiti and B. N. Mandal, Wave scattering by a thin vertical barrier submerged beneath an ice-cover in deep water, *Applied Ocean Research*, **32**(2010), 367–373.

10. S.R. Manam, Scattering of membrane coupled gravity waves by partial vertical barreirs, *ANZIAM Jl*, **51**(2009), 241–260.

11. S. R. Manam, J. Bhattacharjee and T. Sahoo, Expansion formulae in wave structure interaction problems, *Proc. R. Soc. A*, **462**(2006), 263–287.

12. S. R. Manam and R. B. Kaligatla, Effect of a submerged vertical barrier on flexural gravity waves, *Int. Jl. Engg. Sci.*, **49**(2011), 755–767.

13. S. R. Manam and M. Sivanesan, A note on the explicit solutions for wave scattering by vertical porous barriers, *Wave Motion*, **69**(2017), 81–90.

14. R. Mondal and T. Sahoo, Wave structure interaction problems for two-layer fluids in three dimensions, *Wave Motion*, **49(5)**(2012), 501–524.

15. R. Mondal and T. Sahoo, Wave structure interaction problems in three-layer fluid, *Z. Angew. Math. Phys.*, **65**(2014), 349–375.

16. H. Ohta, T. Torii, N. Hayashi, E. Watanabe, T. Utsunomiya, K. Sekita and S. Sunahara, Effect of attachment of a horizontal/vertical plate on the wave response of a VLFS, In: Ertekin RC, Kim JW, editors. *Proc 3rd Int WkspVery Large Floating Structures*, University of Hawaii at Manoa, Honolulu, Hawaii, USA.(1999) pp.265–274.

17. K. Takagi, K. Shimada and T. Ikebuchi, An anti-motion device for a very large floating structure, *Marine Structures*, **13**(2000), 421–436.

18. E. Watanabe, T. Utsunomiya, M. Kuramoto, H. Ohta, T. Torii and N. Hayashi, Wave response analysis of VLFS with an attached submerged plate, *Proc. 12th Int. Offshore Polar Eng.*, Kita-kyushu, Japan, (2002), pp. 319–326.

19. E. Watanabe, T. Utsunomiya, H. Ohta and N. Hayashi, Wave response analysis of VLFS with an attached submerged plate: verification with 2-D model and some 3-D numerical examples, *Proc. Int. Symp. Ocean Space Utilisation Technol.*, National Maritime Research Institute, Tokyo, Japan, (2003), pp. 147–154.

20. X. Yu and A. T. Chwang, Wave motion through porous sturctures, *Journal of Engineering Mechanics*, **120(5)**(1994), 989–1008.

Appendix

$$
\begin{aligned}
J_1(x) &\equiv \int_0^a \frac{e^{xt}}{\sqrt{a^2-t^2}}dt = \frac{\pi}{2}[I_0(ax)+L_0(ax)], \\
J_2(x) &\equiv \int_0^a \frac{t^2e^{xt}}{\sqrt{a^2-t^2}}dt = \frac{a^2\pi}{2}[I_0(ax)+L_0(ax)] - \frac{a\pi}{2x}[I_1(ax)+L_1(ax)], \\
J_3(x) &\equiv \int_a^\infty \frac{e^{xt}}{\sqrt{t^2-a^2}}dt = K_0(-ax), \\
J_4(x) &\equiv \int_a^\infty \frac{t^2e^{xt}}{\sqrt{t^2-a^2}}dt = -\frac{a}{x}K_1(-ax) + a^2K_0(-ax), \\
J_5(x) &\equiv \int_0^a \frac{te^{xt}}{\sqrt{(a^2-t^2)}}dt = a + \frac{a\pi}{2}[I_1(ax)+L_1(ax)], \\
J_6(x) &\equiv \int_a^\infty \frac{te^{xt}}{\sqrt{t^2-a^2}}dt = aK_1(-ax),
\end{aligned}
$$

where K_0, K_1, I_0, I_1 are the modified Bessel functions and L_0, L_1 are the Struve functions.